Supplement of Clim. Past, 15, 2019–2030, 2019
https://doi.org/10.5194/cp-15-2019-2019-supplement

Climate of the Past
Open Access
EGU

Supplement of

Holocene atmospheric iodine evolution over the North Atlantic

Juan Pablo Corella et al.

Correspondence to: Alfonso Saiz-Lopez (a.saiz@csic.es)

Supplementary Information text

Iodine post-depositional processes in Renland snow and ice.

Certain post-depositional remobilization of iodine trapped in snow and ice is expected to occur in ReCAP site since this element can be photo-activated and released from the snowpack in polar regions (e.g. *Frieß et al., 2010; Spolaor et al, 2014, 2019*). Therefore, an adequate characterization of all the post-depositional effects affecting the downcore iodine trend in ReCAP ice core is needed.

Laboratory experiments have shown two photo-induced mechanisms for the release of inorganic iodine from the surface snow to the atmosphere; i) production of I_2 and tri-iodide (I_3^-) through the photo-oxidation of iodide (*Kim et al.*, 2016), and ii) the heterogeneous photo-reduction of iodate and subsequent release of a gas phase photofragment (*Gálvez et al.*, 2016). Field studies addressing iodine remobilization after snow deposition has been conducted in Antarctica (*FrieB et al. 2000; Spolaor et al. 2014*), Europe (*Legrand et al., 2018*) and in the Arctic (*Spolaor et al., 2019*). According to these field experiments iodine recycling in surface snow depends on the season and amount of incoming radiation. Maximum iodine levels in ice are found in winter due to limited biological production and the absence of photochemistry (*Frieb et al., 2010; Spolaor et al., 2014*) although night-time radical activation could also occur *(Saiz-Lopez et al., 2016*). A very recent field experiment on the diurnal cycle of iodine in surface snow in the Arctic has revealed for the first time the behaviour of iodine in the upper snow layers (0-3 cm) under different light and atmospheric conditions (*Spolaor et al., 2019*). Iodine is found to be very active in the upper snow layer with the highest iodine concentration measured at night and the lowest during the day (*Spolaor et al., 2019*). Daytime iodine snow-re-emissions would rapidly form reservoir species (HOI, IONO2, HI) redepositing back to snow once photochemistry ceases during the night-time. Therefore, the recycling of iodine on ice and snow surfaces on a daily to seasonal scale only represents an offset change affecting the effective atmospheric lifetime of iodine against deposition (*Saiz-Lopez et al.*, 2014) which would not affect the net iodine depositional fluxes and concentrations at decadal to

millennial time scales. In Greenland, solar irradiation maxima is found during the HTM (*Laskar et al. 2004*) (Fig. 2) that would result in higher re-emission of surface snow iodine to the atmosphere during that period. Thus, the highest iodine values measured in this period suggest that iodine loss is not a major driver for the recorded iodine variability. Additionally, neither the iodine trend during the HTM nor the abrupt changes in iodine concentration and fluxes found during the HTM/Neoglacial transitions follows the solar irradiance evolution throughout the Holocene (Fig. 2) suggesting that long-term solar irradiance have not controlled the Holocene iodine concentrations in RECAP ice core.

Iodine release from the snow-pack in Greenland is particularly higher at low snow accumulation sites, where iodine loss from the surface snow could be one order of magnitude higher (*Maselli et al., 2017; Legrand et al., 2018*). Losses of volatile iodine species would be strongly reduced in areas with high annual snow accumulation rates such as the Renland peninsula (annual snow accumulation rates ca. 500 kg m^{-2} yr^{-1}; Fig. S2). Thus, the high accumulation rates found in ReCAP (Fig. 2) may limit the post-depositional remobilization of high volatile iodine species throughout the Holocene. In the ReCAP ice core, the reconstructed accumulation rates shown in Figure S2 shows reasonably stable levels for the last 8000 years, suggesting relatively constant snowfall and surface conditions. The absence of any significant correlation between the accumulation rates and the concentration of impurities such as iodine and sodium also indicate that the Holocene iodine variability in ReCAP ice core is neither related to the effects of changing snow deposition rates nor to meteorological conditions in Renland Peninsula. A systematic decrease in iodine content has been recently reported in firn ice in different Greenland sites with density values <0.83 g cm^{-3} (*Legrand et al., 2018*) suggesting possible iodine volatilization during firn storage or melting. Nevertheless, this study is based on dense ice with density values >0.89 g cm^{-3} where the air bubbles trapped are well sealed that minimize loss of iodine during analyses.

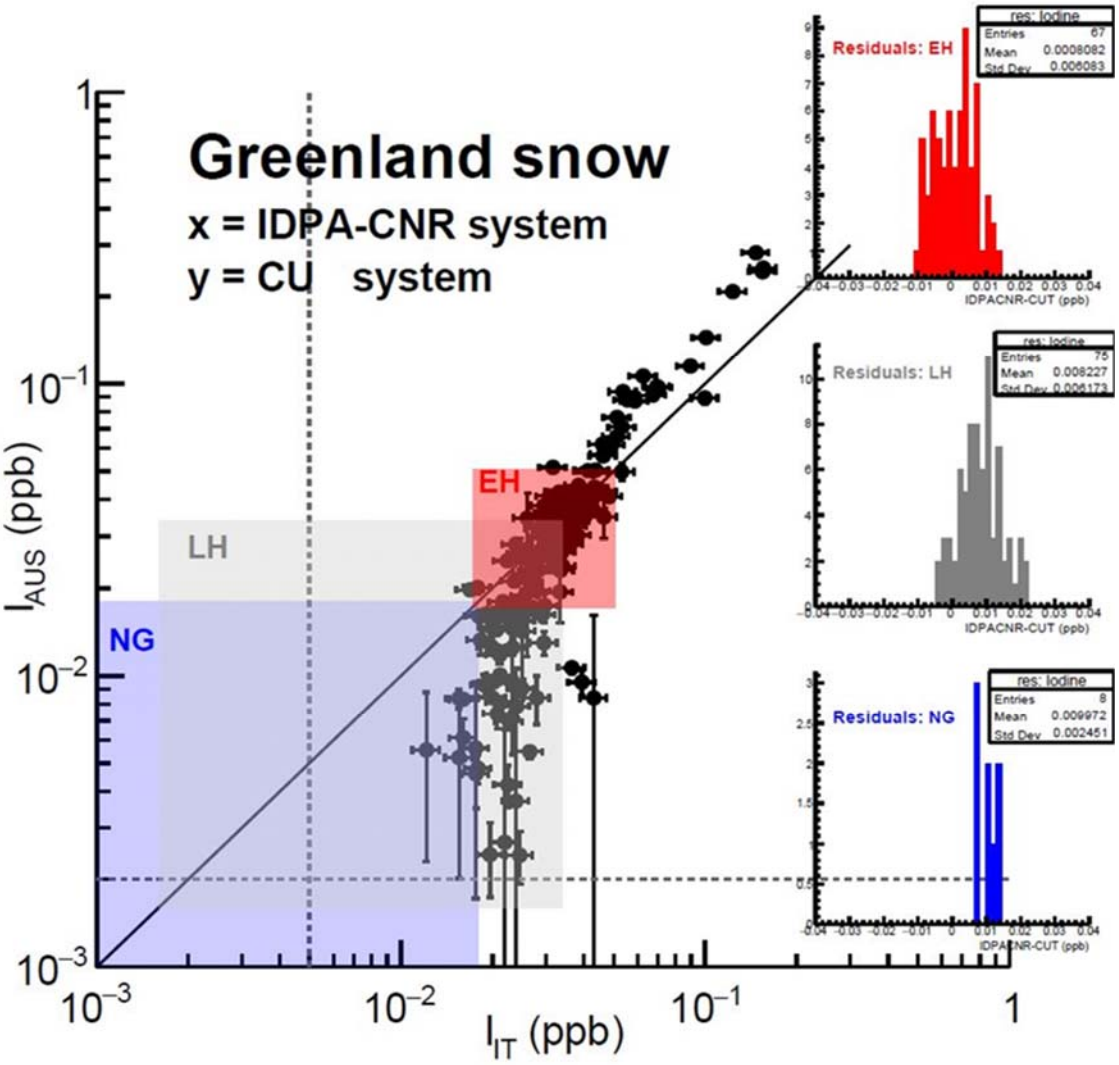

Figure S1: Iodine intercalibration between the IDPA-CNR (Venice, Italy) and the CU (Perth, Australia) systems performed on Greenland surface snow iodine measurements. The colored areas reflect the average (± 2σ) iodine concentrations detected in the RECAP ice core (EH: Early Holocene; NG: Neoglacial Period; LH: Late Holocene).

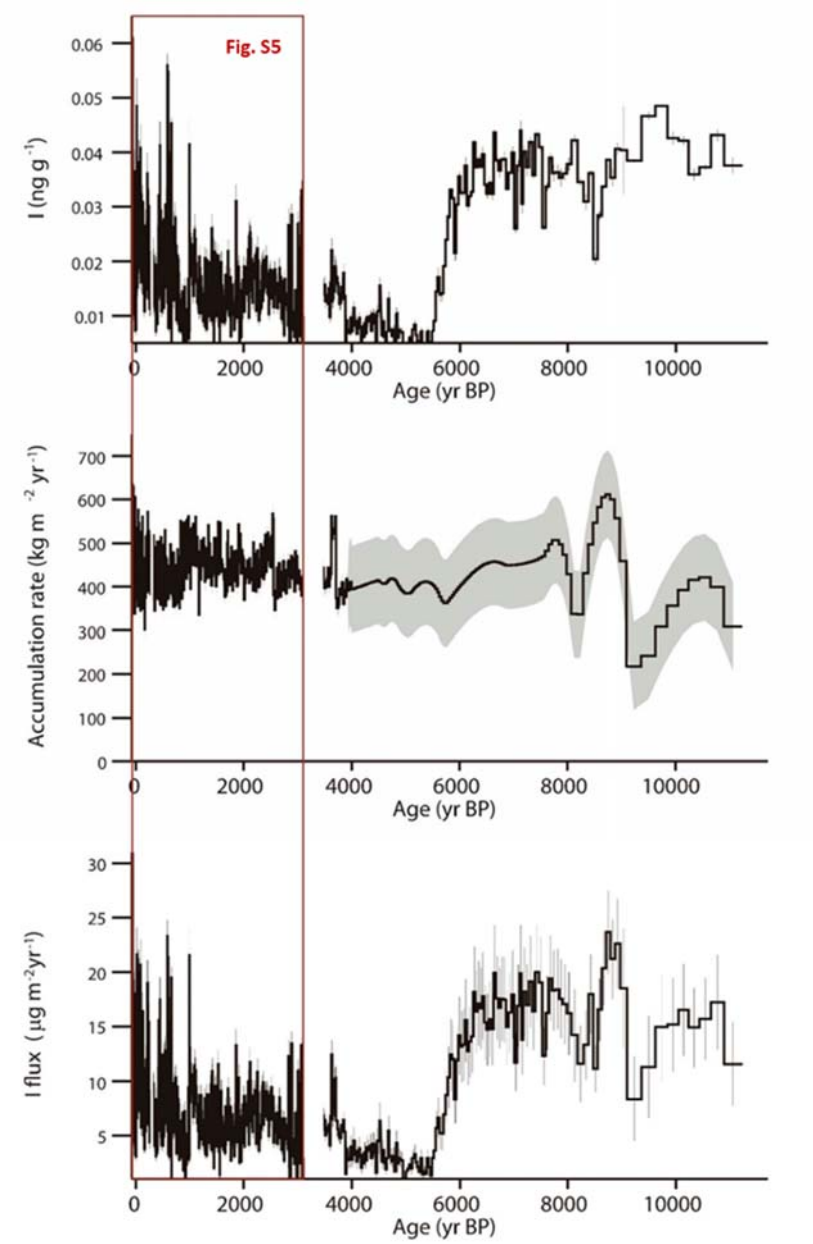

Figure S2. ReCAP ice core time series during the Holocene: Top: iodine concentration (1σ, experimental uncertainties). Middle: accumulation rates and associated uncertainties (1σ band). Bottom: iodine fluxes (1σ, propagated from the concentration and accumulation rate uncertainties). Iodine measurements are missing for the time intervals 275-320 yr BP and 3107-3476 yr BP due to instrumental errors during the analyses. The brown inset area is shown in Fig S5.

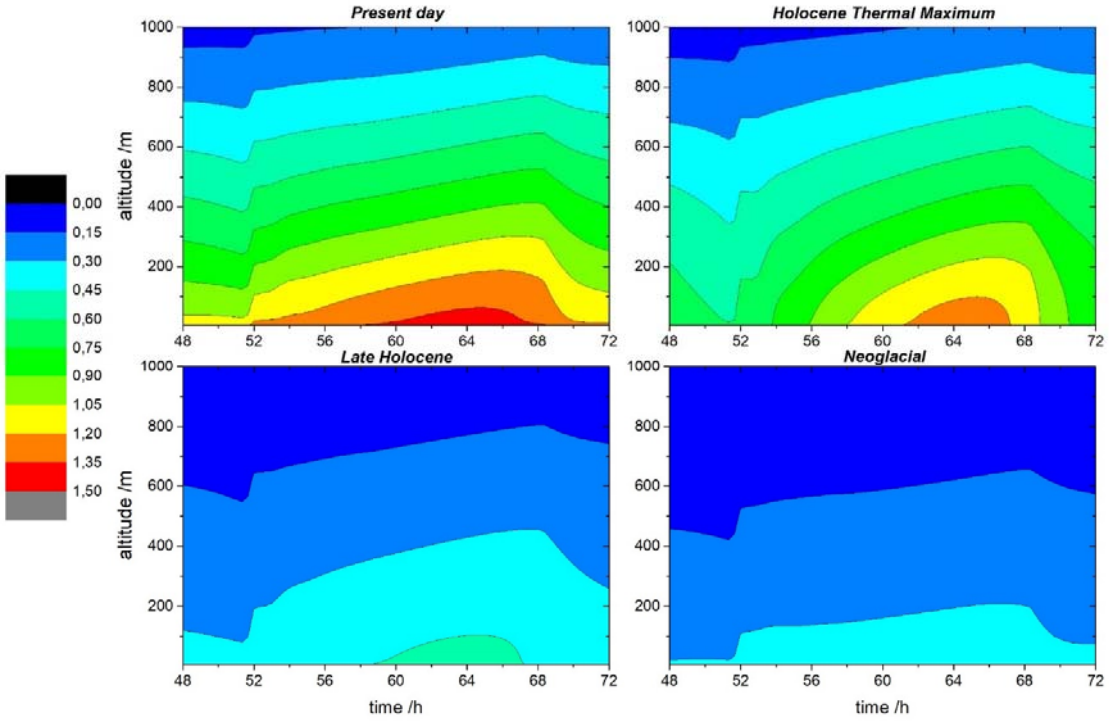

Figure S3. Diurnal variation of reactive iodine modelled by THAMO in different scenarios of $[O_3]$ and VSLs e missions fluxes (Table 1) from i) present day (top left) : $[O_3]$= 30 ppbv and present day VSL emission fluxes; ii) Holocene Thermal Maximum (top right): $[O_3]$ = 10 ppbv and 100% increase in present day VSL emission fluxes; iii) Late Holocene (bottom left): $[O_3]$ = 10ppbv and 50% decrease in present day VSL emission fluxes; iv) Neoglacial (bottom right): $[O_3]$ = 10 ppbv and 87% decrease in present day emission fluxes. I_y comprises I_2+IO+HOI+HI+INO_2+INO_3

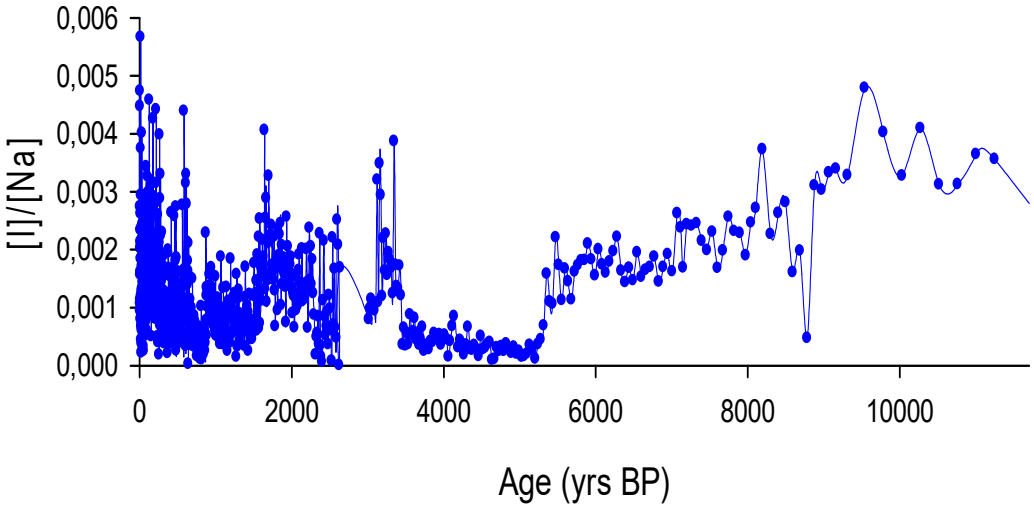

Fig. S4: **ReCAP ice core iodine to sodium concentration ratio during the Holocene**

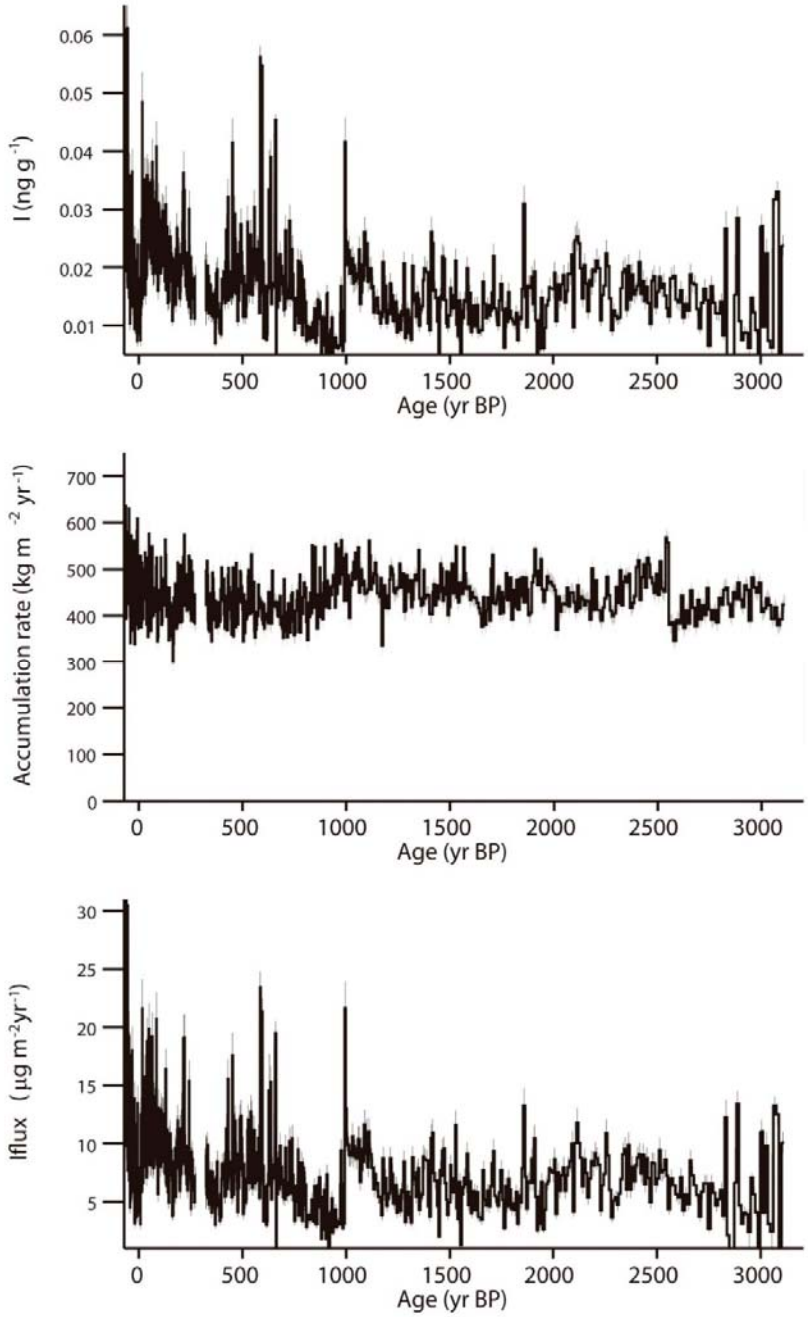

Fig. S5: **ReCAP ice core time series during the Late Holocene**: Top: iodine concentration (1σ, experimental uncertainties). Middle: accumulation rates (and 1σ uncertainties). Bottom: iodine fluxes (1σ, propagated from the concentration and accumulation rate uncertainties).

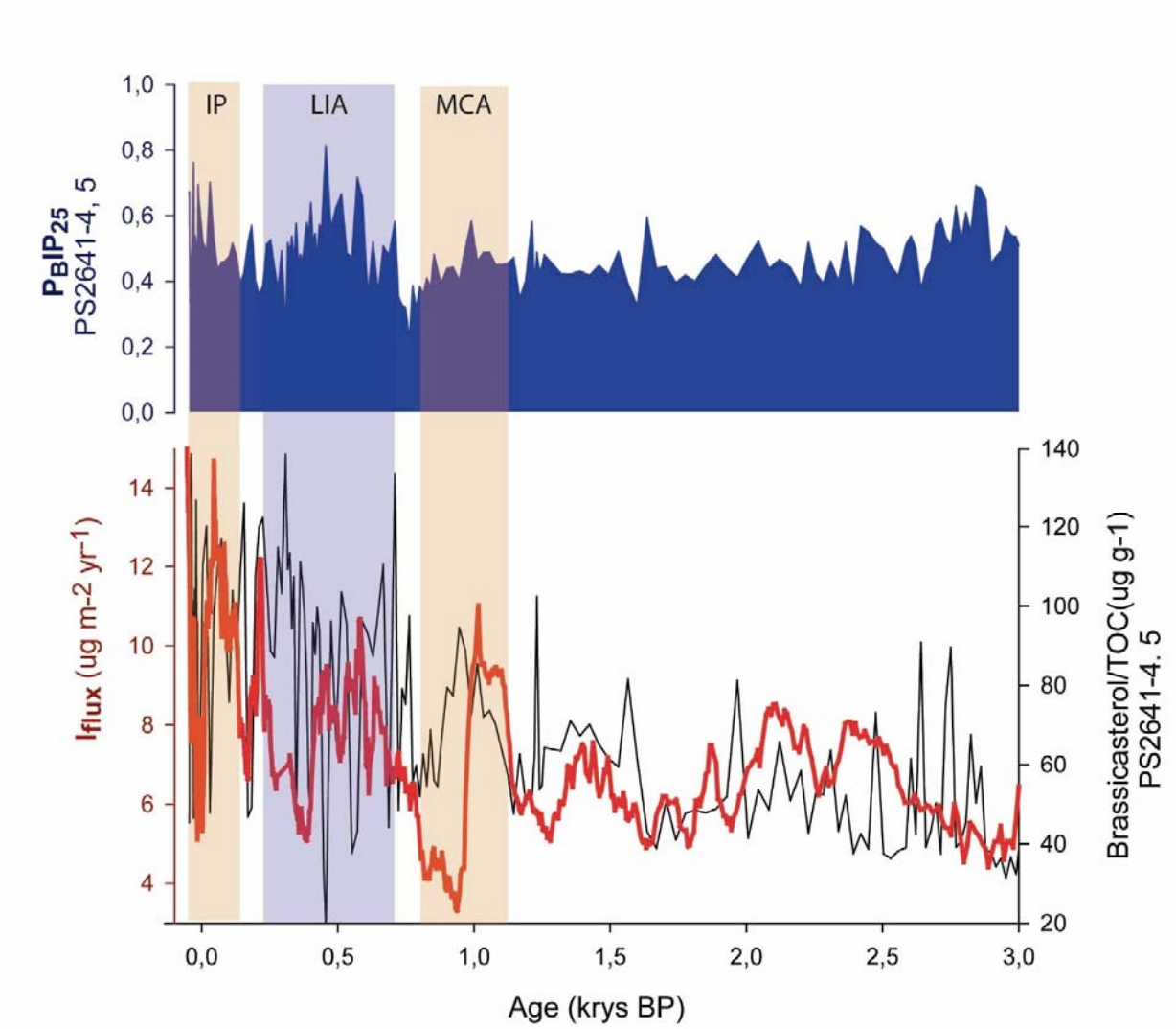

Fig. S6: **ReCAP ice core fluxes, primary productivity and sea-ice conditions in Eastern Greenland during the Late Holocene**: Bottom: I_{flux} 10-samples running average in ReCAP ice core (red) and *Brassicasterol* in eastern Greenland coastal shelf (core PS2641-4,5) (black) (*Kolling et al.*, 2017). Top: eastern Greenland coastal shelf sea-ice extent proxy P_BIP_{25} (*Kolling et al.*, 2017). Color bars indicate the last millennium main climatic phases (LIA: Little Ice Age; MCA; Medieval Climate Anomaly; IP: Industrial Period).

	Holocene Thermal Maximum	Neoglacial	Late Holocene	HTM/ Neoglacial transition
[I] (ng/g)	**0.034**	**0.009**	**0.018**	**277%**
std	*0.01*	*0.00*	*0.01*	
I_{flux} (ug/m^2 yr)	**14.75**	**3.97**	**8.02**	**271%**
std	*4.38*	*2.16*	*4.09*	
Planktic foraminifera (ind/cm^2 kyr)	**6270**	**3653**	**5041**	**71.6%**
std	*4066*	*1365*	*2173*	
***Brassicasterol* (ug/g OC)**	**36.43**	**31.85**	**36.74**	**14.4%**
std	*7.69*	*4.13*	*5.30*	
Dinosterol (%)	**4.69**	**2.98**	**4.86**	**57.4%**
std	*2.40*	*0.67*	*1.58*	
T. Quinqueloba (%)	**32.87**	**19.35**	**21.83**	**70%**
std	*13.87*	*6.44*	*9.64*	
Arctic SST (ºC)	**10.40**	**9.81**	**9.88**	**6%**
std	*0.77*	*0.39*	*0.30*	
P_DIP_{25}	**0.09**	**0.19**	**0.30**	**-52.6%**
std	*0.05*	*0.02*	*0.08*	
IP_{25}	**0.14**	**0.84**	**1.52**	**-83.3%**
std	*0.17*	*0..31*	*0.69*	
71ºN July solar irradiance (W/m^2)	**519.17**	**493..69**	**487..57**	**5.2%**
std	*3.28*	*3.93*	*5.24*	

Table S1: Mean values and standard deviations (1 std) of iodine levels (iodine concentration and fluxes) in ReCAP ice core and mean values of environmental proxies reconstructed in the Arctic during the main climatic periods discussed in the text (i.e. Holocene Thermal Maximum, Neoglacial period and Late Holocene). From bottom to top: Iodine concentrations [I]; Iodine fluxes (I_{flux}); Planktic foraminifera (*Telesiński et al.*, 2015; *Werner et al.*, 2013); *Brassicasterol* and *dinosterol* (*Kolling et al.*, 2017; *Müller et al.*, 2012; *Werner et al.*, 2016); *T. quinqueloba* (Werner et al., 2013; Telesinski et al., 2015*)*; Sea surface temperature (SST) (*Bendle and Rosell-Melé*, 2004; *Justwan and Koç*, 2008; *Justwan et al.*, 2008); Sea-ice cover (P_DIP_{25} and IP_{25}) (*Cabedo-Sanz et al.*, 2016; *Werner et al.*, 2016; *Xiao et al.*, 2017); **i)** 71ºN July solar irradiance (*Laskar et al.*, 2004).

	A) Great Acceleration *(1950-Present-day)*	
	[Na]	[Ca]
[I]	0.252*	
Sig	*0.026*	
N	*78*	
	B) Late Holocene *(last 3.4 kyrs BP)*	
	[Na]	[Ca]
[I]	0.095*	*0.215**
Sig	*0.011*	*0.030*
N	*717*	*102*
	C) Neoglacial *(5.5-3.4 kyrs b2k)*	
[I]	**-0.42****	
Sig	0.000	
N	75	
	D) HTM *(11.7-5.5 kyrs BP)*	
[I]	-0.228	-0.009
Sig	*0.062*	*0.943*
N	*68*	*68*

(ρ=Pearson correlation coefficient, Sig=significance (*=significance<0.05, **=significance<0.01 highlighted in bold font)

Table S2. Great Acceleration, Late Holocene, Neoglacial and Holocene Thermal Maximum Pearson (ρ) correlation coefficients between iodine concentrations [I] in the Renland ice core and sodium [Na] and calcium [Ca] concentrations. [Ca] data are not available for the Great Acceleration and the Neoglacial Period.

References:

Bendle, J.A.P., A. Rosell-Melé, High-resolution alkenone sea surface temperature variability on the North Icelandic Shelf: implications for Nordic Seas palaeoclimatic development during the Holocene. The Holocene 17, 9-24 (2007).

Cabedo-Sanz, P., Belt, S. T., Jennings, A. E., Andrews, J. T. and Geirsdóttir, Á., Variability in drift ice export from the Arctic Ocean to the North Icelandic Shelf over the last 8000 years: a multi-proxy evaluation, Quaternary Science Reviews, 146, 99-115, 2016.

Frieß, U., Deutschmann, T., Gilfedder, B., Weller,R., and Platt, U.: Iodine monoxide in the Antarctic snowpack, Atmospheric Chemistry and Physics, 10, 2439-2456, 2010

Gálvez, Ó., Baeza-Romero, M. T., Sanz, M. and Saiz-Lopez, A., Photolysis of frozen iodate salts as a source of active iodine in the polar environment. Atmospheric Chemistry and Physics 16, 12703-12713, 2016.

Justwan, N. Koç, A. E. Jennings, Evolution of the Irminger and East Icelandic Current systems through the Holocene, revealed by diatom-based sea surface temperature reconstructions. Quaternary Science Reviews 27, 1571-1582, 2008.

Justwan, A., N. Koç, A diatom based transfer function for reconstructing sea ice concentrations in the North Atlantic. Marine Micropaleontology 66, 264-278 (2008).

Kim, K., Yabushita, A., Okumura, M., Saiz-Lopez, A., Cuevas, C. A., Blaszczak-Boxe, C. S., Min, D., W. Yoon, H.-I. and Choi, W., Production of molecular iodine and tri-iodide in the frozen solution of iodide: implication for polar atmosphere, Environmental science & technology, 50(3), 1280-1287, 2016.

Kolling, H. Stein, M., R., Fahl, K., Perner, K. and Moros M., Short-term variability in late Holocene sea ice cover on the East Greenland Shelf and its driving mechanisms, Palaeogeography, Palaeoclimatology, Palaeoecology, 485, 336-350, 2017.

Laskar, J., P. Robutel, F. Joutel, M. Gastineau, A. Correia, B. Levrard, A long-term numerical solution for the insolation quantities of the Earth. Astronomy & Astrophysics 428, 261-285, 2004.

Legrand, M., McConnell, J. R., Preunkert, S., Arienzo, M., Chellman, N., Gleason, K., Sherwen, T., Evans, M. J., and Carpenter, L. J.: Alpine ice evidence of a three-fold increase in atmospheric iodine deposition since 1950 in Europe due to increasing oceanic emissions, Proceedings of the National Academy of Sciences, 115, 12136-12141, 2018

Maselli, O. J., Chellman, N. J., Grieman, M., Layman, L., McConnell, J. R., Pasteris, Daniel, Rhodes, R.l H., Saltzman, E. and Sigl, M.l. Sea ice and pollution-modulated changes in Greenland ice core methane sulfonate and bromine. Climate of the Past, 13 (1). pp. 39-59. 2017

Müller, J., Werner, K., Stein, R., Fahl, K., Moros, M. and Jansen, E., Holocene cooling culminates in sea ice oscillations in Fram Strait, Quaternary Science Reviews, 47, 1-14, 2012.

Saiz-Lopez, A., Fernandez, R. P., Ordóñez, C., Kinnison, D. E., Gómez Martín, J. C., Lamarque, J. F., and Tilmes, S. Iodine chemistry in the troposphere and its effect on ozone. Atmospheric Chemistry and Physics, 14(23), 13119-13143. 2014.

Saiz-Lopez, a., J. M. C. Plane, C. A. Cuevas, A. S. Mahajan, J. F. Lamarque, D. E. Kinnison, Nighttime atmospheric chemistry of iodine. Atmos. Chem. Phys. 16, 15593-15604, 2016.

Spolaor, A., P. Vallelonga, J. Gabrieli, T. Martma, M. P. Björkman, E. Isaksson, G. Cozzi, C. Turetta, H. A. Kjær, M. A. J. Curran, A. D. Moy, A. Schönhardt, A. M. Blechschmidt, J. P. Burrows, J. M. C. Plane and C. Barbante. Seasonality of halogen deposition in polar snow and ice. Atmos. Chem. Phys. 14: 9613-9622. 2014.

Spolaor, A., Barbaro, E., Cappelletti, D., Turetta, C., Mazzola, M., Giardi, F., Björkman, M.P., Lucchetta, F., Dallo, F., Pfaffhuber, K.A., Angot, H., Dommergue, A., Maturilli, M., Saiz-Lopez, A., Barbante, C. and Cairns, W.R.L. Diurnal cycle of iodine and mercury concentrations in Svalbard surface snow. Atmos. Chem. Phys. Discuss. 2019, 1-25. 2019

Telesiński, M., Bauch, H. A., Spielhagen, R. F. and Kandiano E. S., Evolution of the central Nordic Seas over the last 20 thousand years, Quaternary Science Reviews, 121, 98-109, 2015.

Werner, K., Spielhagen, R. F., Bauch, D., Hass, H. C. and Kandiano, E., Atlantic Water advection versus sea-ice advances in the eastern Fram Strait during the last 9 ka: Multiproxy evidence for a two-phase Holocene, Paleoceanography, 28(2), 283-295, 2013.

Werner, K., Müller, J., Husum, K., Spielhagen, R. F., Kandiano, E. S. and Polyak, L., Holocene sea subsurface and surface water masses in the Fram Strait–Comparisons of temperature and sea-ice reconstructions, Quaternary Science Reviews, 147, 194-209, 2016.

Xiao, X., Zhao, M., Knudsen, K. L., Sha, L., Eiríksson, J., Gudmundsdóttir, E., Jiang, H. and Guo, Z., Deglacial and Holocene sea–ice variability north of Iceland and response to ocean circulation changes, Earth and Planetary Science Letters, 472, 14-24, 2017.